Published in final edited form as:
Angew Chem Int Ed Engl. 2010 July 19; 49(31): 5362–5366. doi:10.1002/anie.201001675.

Porous Metal Carboxylate Boron Imidazolate Frameworks (MC-BIFs)

Dr. Shoutian Zheng,
Department of Chemistry and Biochemistry, California State University, Long Beach, 1250 Bellflower Boulevard, Long Beach, CA 90840

Tao Wu,
Department of Chemistry, University of California, Riverside, CA 92521

Dr. Jian Zhang,
Department of Chemistry and Biochemistry, California State University, Long Beach, 1250 Bellflower Boulevard, Long Beach, CA 90840

Mina Chow,
Department of Chemistry and Biochemistry, California State University, Long Beach, 1250 Bellflower Boulevard, Long Beach, CA 90840

Ruben A. Nieto,
Department of Chemistry and Biochemistry, California State University, Long Beach, 1250 Bellflower Boulevard, Long Beach, CA 90840

Prof. Dr Pingyun Feng, and
Department of Chemistry, University of California, Riverside, CA 92521

Prof. Dr Xianhui Bu
Department of Chemistry and Biochemistry, California State University, Long Beach, 1250 Bellflower Boulevard, Long Beach, CA 90840, Fax: (+) 562-985-8557

Pingyun Feng: pingyun.feng@ucr.edu; Xianhui Bu: xbu@csulb.edu

Abstract

Integrated Material for Efficient CO_2 Storage A new family of porous materials with tunable gas sorption properties have been made by integrating metal carboxylates and boron imidazolates under hydro- or solvothermal conditions. One hydrothermally synthesized phase exhibits a very high volumetric CO_2 storage capacity at 81 L/L (273K, 1atm).

Keywords

Porous; Metal-organic framework; Carboxylate; Boron; Imidazolate

Metal-organic frameworks (MOFs) have attracted considerable interest because of their intriguing structures and potential applications.[1] Of particular importance is the design and synthesis of MOFs with novel composition and topology, because properties and applications of such materials depend on their unique composition and topology. Among MOFs, metal-carboxylate frameworks (MCFs) constitute one of the most important subclasses and have been studied extensively.[2–6] Some well-known porous MCFs include

Correspondence to: Pingyun Feng, pingyun.feng@ucr.edu; Xianhui Bu, xbu@csulb.edu.

Supporting information for this article is available on the WWW under http://www.angewandte.org or from the author.

HKUST-1,[3a] MOF-5,[3b] and MIL-101.[3c] In addition to MCFs, porous frameworks constructed from heterocyclic ligands (e.g., zeolitic imidazolate frameworks, ZIFs) and di- and trivalent cations such as Zn^{2+} and In^{3+},[7,8] have also been developed. More recently, boron imidazolate frameworks (BIFs) based on boron imidazolate complexes were reported.[9] Ultra-lightweight elements such as B and Li (e.g., in BIF-9 with the zeolite RHO net), together with the strong covalent bond (B-N) hold promise for the development of stable low-density porous solids with potential applications such as on-board gas storage materials.

In MCFs, ZIFs, and BIFs, crosslinking ligands (carboxylates, imidazolates, and boron imidazolates, respectively) have different properties, leading to porous frameworks with distinct structural features and properties. Here, we are interested in unifying these different structural modes in the same framework to create a family of materials called metal carboxylate boron imidazolate frameworks (MC-BIFs). Such a multi-component system can lead to greater compositional and topological diversity. As a first step, divalent metal ions widely used for MCFs and ZIFs are chosen for this work, because M^{2+} ions have a strong affinity for both carboxylates and imidazolates, making it possible to combine carboxylate and $[B(im)_4]^-$ inthe same framework without phase separation.

Another consideration involves the local charge distribution and overall charge of the target framework. Since $[B(im)_4]^-$ readily forms neutral zeolite-type frameworks with monovalent Li and Cu ions (e.g., $LiB(im)_4$), the combination of higher charged metal ions such as Zn^{2+} with $[B(im)_4]^-$ would likely result in positively charged structural subunits (chains, layers, or even 3D frameworks). The introduction of di- or polycarboxylates with a higher charge density (2-, -3, … per ligand) than imidazolates (−1 per ligand) can provide charge compensation for the positively charged $M^{2+}/[B(im)_4]^-$ subunits, leading to the formation of neutral MC-BIFs.

Here, we report a family of MC-BIFs that integrate both carboxylate and imidazolate building blocks. MC-BIF-1S through MC-BIF-5H all possess 3D framework structures, while MC-BIF-6S has a 3-connected ladder-like structure. Noteworthy is the use of both hydro- and solvothermal conditions in this work. MOFs are generally prepared under solvothermal conditions and many have limited hydrothermal stability. Since the hydrothermal stability is key to some applications of MOFs, it has been desirable to synthesize MOFs under hydrothermal conditions. Here, MC-BIF-1S, MC-BIF-4S, and MC-BIF-6S were solvothermally synthesized while MC-BIF-2H, MC-BIF-3H, and MC-BIF-5H were made by hydrothermal synthesis.

Chiral MC-BIF-1S is the first example that integrates the bonding features in all three families of materials (i.e., MCFs, ZIFs, and BIFs). Despite such a complex composition, its topology is very simple. One fundamental feature of MC-BIF-1S is the pentagonal layer parallel to the *ab*-plane (Figure 1a). Within the layer, only pentagonal rings consisting of two B and three Zn sites are observed, and each Zn^{2+} site is bonded to two $[B(im)_4]^-$ complexes and one free im ligands (“free” means that this imidazolate ligand is not a part of the covalent $[B(im)_4]^-$ complex). Each boron site is 4-connected to four separate Zn sites.

The aforementioned pentagonal layer was previously observed in ZBIF-1 with the formula of $Zn_2(im)Cl_2[B(im)_4]$.[10] However, because of the rich chloride environment in the deep eutectic solvent (choline chloride/N,N′-dimethylurea) used for the synthesis of ZBIF-1, the fourth Zn^{2+} coordination site in ZBIF-1 is terminated by Cl^-, leading to an overall lamella structure. By replacing terminal Cl^- anions with crosslinking ligands, it should be possible to convert 2D ZBIF-1 into a 3D framework. In this work, we have identified a unique crosslinker-solvent combination that allowed us to achieve this goal. By eliminating the Cl^-

source and employing a unique solvent, 1,3-dimethyl-propyleneurea, the B/im/Zn pentagonal layers have been pillared through Zn-bdc-Zn linkages (Table 1) into a 3D framework called MC-BIF-1S here (Figure 1b).

MC-BIF-2H illustrates the effect of solvents on the self-assembly process in the Zn-$[B(im)_4]$-bdc system. Compared to MC-BIF-1S, one notable difference is that the free imidazolate ligand (in the form of Zn-im-Zn) is no longer present, suggesting the possible lower hydrothermal stability the M(II)-im-M(II) linkage, as compared to the M(II)-im-B(III) linkage. Another difference is the coordination of water to one of two unique Zn sites, an obvious effect of the hydrothermal synthesis (Figure S2). Each Zn1 ion is coordinated to four im ligands and one water molecule to form a distorted trigonal bipyramidal configuration, while each Zn2 ion is tetrahedrally bonded to two im ligands and two O donors from two bdc ligands. As shown in Figure 1c, two Zn1 ions are bridged together by two $[B(im)_4]^-$ groups to form a four-ring, which further extends into a 1D B/im/Zn chain by sharing zinc corners. Next, each 1D Zn/$[B(im)_4]^-$ chain is connected to four adjacent chains via Zn2 ions to yield a 3D Zn/$[B(im)_4]^-$ framework with 1D channels in which the bdc ligands are located (Figure 1d, S3). Such bdc ligands bridge Zn2 ions by completing their two remaining coordination sites. It is worth noting that even without considering crosslinking by dicarboxylates, the connectivity between Zn^{2+} and $[B(im)_4]^-$ alone is 3D.

MC-BIF-1S and MC-BIF-2H demonstrate the feasibility to synthesize MC-BIFs under hydrothermal or solvothermal conditions. We then further examined the versatility of our synthetic method by expanding from the dicarboxylate system to the tricarboxylate system, leading to the hydrothermal synthesis of MC-BIF-3H. Again, as in MC-BIF-2H, there is no M(II)-im-M(II) in MC-BIF-3H, consistent with our earlier observation of possibly higher hydrothermal stability of M(II)-im-B than that of M(II)-im-M(II).

MC-BIF-3H can be considered as built from the 2D B/im/Zn layer pillared by the carboxylate ligands. There are two unique tetrahedral zinc sites (Figure S4), which are bonded to two N and two O atoms from two im and two btc ligands. MC-BIF-3H consists of two types of macrocyclic $B_4Zn_4(im)_8$ eight-rings (Figure S5): one is a square-type eight-ring and the other is an elongated narrow-type eight-ring. Every square-type eight-ring shares its four edges with four narrow-type eight-rings, and vice versa, resulting in 2D Zn/$[B(im)_4]$ layers that are further linked by btc ligands to yield a 3D structure (Figure 1e).

When using mixed crosslinking ligands, their ratio and the role of each ligand in determining the dimensionality of the overall framework are of significance in the control of framework composition and topology. As discussed above, in MC-BIF-1S and MC-BIF-3H, the M^{2+}/im/B connectivity is 2D and the connectivity in the third dimension is established by bridging carboxylate ligands. In comparison, MC-BIF-2H possesses the 3D M^{2+}/im/B connectivity with the charge-balancing carboxylate ligand completing the remaining Zn coordination sites.

Here we demonstrate that the competing role of different ligands (i.e., carboxylates and imidazolates) can be tuned. Specifically, it is possible to broaden the dimensionality of M^{2+}/im/B connectivity to include 1D, and in the meantime to increase the dimensionality of the M^{2+}/carboxylate connectivity. Such a change in the dimensionality of the metal-ligand substructure connectivity is generally accompanied by a change in the carboxylate/$B(im)_4^-$ ratio within the framework. Here, the use of a metal ion (Cd^{2+} in this work) with the ionic radius larger than Zn^{2+} offers an insight into the correlation between the overall structure and its atomic building block.

The use of Cd^{2+} to vary the carboxylate/$B(im)_4^-$ ratio and to tune the dimensionality of M^{2+}/carboxylate and M^{2+}/B/im substructures can involve the following two factors: (1) the

carboxylate can be the chelating ligand whereas $[B(im)_4]^-$ can not; (2) because of the larger ionic radius, Cd^{2+} has a greater tendency to form a chelate than Zn^{2+}. These two factors are likely the reason for the increased carboxylate/$B(im)_4^-$ ratio and a reduction in the M^{2+}/im/B connectivity to 1D in two new MC-BIFs made with Cd^{2+} (in all zinc compounds here, the carboxylate/$B(im)_4^-$ ratio = 1).

MC-BIF-4S and MC-BIF-5H, in which the carboxylate/$B(im)_4^-$ ratio is 1.5 and 2, respectively, are constructed from 1D $Cd^{2+}/[B(im)_4]^-$ tubes linked by bdc ligands into 3D structures. In MC-BIF-4S, there are two unique Cd sites (Figure S6). The 6-coordinate Cd1 only serves as a 3-connected node to two B atoms and one Cd atom *via* two im ligands (non-chelating) and one bdc ligand (chelating), respectively. There are two terminal ligands, one Him and one p-murea. The 5-coordinate Cd2 acts as a 4-connected node crosslinked to two B atoms and two Cd atoms *via* two im ligands and two bdc ligands, respectively. Thus, the 3D structure of MC-BIF-4S can be described as follows. First, as shown in Figure 1f, every two Cd1 ions and two $[B(im)_4]^-$ groups are alternately joined together via Cd-im-B linkages to form a $B_2Cd_2(im)_8$ four-ring. Then, the adjacent four-rings are further bridged by two Cd2 ions along the *a*-axis to generate an infinite B/im/Cd tube. Finally, these tubes are crosslinked along the *b*- and *c*-directions to generate a 3D framework (Figure 1g). This structural feature of MC-BIF-4S is similar to a recently reported zincophosphate constructed from 1D zinc phosphate four-ring columns interlinked by organic ligands.[11]

By switching from solvothermal to hydrothermal method in the Cd system, a new 3D structure MC-BIF-5H was obtained. The structure of 1D B/im/Cd tube in MC-BIF-5H is similar to that in MC-BIF-4S (Figure S7). These B/im/Cd tubes are further joined together via COO^- groups to form a 3D framework (Figure 1h). The effect of hydrothermal synthesis again reveals itself through the inclusion of water molecules in MC-BIF-5H.

From MC-BIF-1S through MC-BIF-5H, the bridging di- or tricarboxylates are used. With the monocarboxylate ligand (acetate in this case), it is possible to obtain crystals that contain isolated low-dimensional M/carboxylate/$B(im)_4$ structures that are potential structural building blocks in higher dimensional structures. One such structure is MC-BIF-6S with a 1D double-chain structure. MC-BIF-6S is made up of $\{[Zn(OAC)_2]_2[B(im)_4]_2\}$ four-rings (Figure 2k). Similar four-ring structures are also observed in MC-BIF-2H, MC-BIF-4S and MC-BIF-5H. However, unlike corner-sharing four-rings in MC-BIF-2H or isolated four-rings in MC-BIF-4S and -5H, four-rings in MC-BIF-6S share edges to form a ladder-type structure.

The total potential solvent accessible volumes of solvothermal products MC-BIF-1S and MC-BIF-4S, calculated with *PLATON*,[12] are 52.2% and 47.8%, respectively. In comparison, the potential solvent accessible volumes of hydrothermal products (MC-BIF-2H: 13.7%; MC-BIF-3H: 18.7%; MC-BIF-5H: 11.3%) are much smaller, which may be related to the size of the solvent molecule. However, as shown below, the actual measured porosity does not correlate with the calculated trend, which is likely caused by the pore geometry and the degree of solvent removal in each case.

Gas adsorption measurements (H_2, CO_2, and N_2) were performed on a Micromeritics ASAP 2010 surface-area and pore-size analyzer, which confirmed the permanent microporosity of MC-BIF-2H, MC-BIF-3H, and MC-BIF-5H (Figure 2). These samples were degassed at 150 °C for 24 h under vacuum prior to the measurement. Figure 2 shows the dependence of gas sorption properties on the crystal structure. The maximum CO_2 adsorptions of MC-BIF-2H, MC-BIF-3H and MC-BIF-5H at 273 K and 1 atm are 54.3, 36.4 and 5.3 cm^3g^{-1}, respectively. The CO_2 uptake capacity, especially the volumetric storage capacity, of MC-BIF-2H (81 L/L) at 1 atm and 273 K is very high, particularly considering its relatively low

percentage of the solvent accessible volume (only 13.7%). Such a high CO_2 storage capacity was further verified by multiple samples made from repeated syntheses and three independent adsorption measurements. In comparison, the volumetric CO_2 storage capacity for ZIF-69 is about 83L/L under the same condition.[13]

To gain insight into the high CO_2 adsorption capacity, thermogravimetric data of MC-BIF-2H are analyzed, which gives the first weight loss (4.66%) in the range 120 ~ 220 °C and no further weight loss up to 300 °C (Figure S11), in good agreement with the removal of both extraframework and terminal water molecules (4.75%). We further examined the water loss and the associated structural change by temperature-dependent single crystal X-ray diffraction. The refinement results show that after heating at 220 °C for 2 hours, the single crystal remains stable and that both extraframework and terminal water molecules can be removed (see ESI), leading to open metal sites on Zn1 (Figure S13).

The open Zn^{2+} site in MC-BIF-2 is different from other M^{2+} sites in the MC-BIF series, because it is bonded to $B(im)_4^-$ complexes while in other structures each M^{2+} site is bonded to at least one carboxylate end. Compared to ZIFs, this open zinc site is also special because the negative charge of four adjacent imidazolate ligands is drawn more toward B^{3+} in MC-BIF-2. It is thus expected that the open Zn^{2+} site in MC-BIF-2 receives less negative charge from adjacent ligands and has a correspondingly higher level of the local positive charge, likely making it more polarizing. The net result is likely an increased interaction with CO_2, leading to an enhanced CO_2 adsorption capacity.[14] Additionally, because of the small kinetic diameter of CO_2, the large pore window or large cage cavity is not essential for efficient adsorption. In MC-BIF-2H, the pore space formed by 3D metal-boron-imidazolate framework is further partitioned by dicarboxylates into smaller pore regions, which may also help enhance the CO_2 storage. This is consistent with the previous observations that interpenetration and extra-framework species can enhance gas sorption properties, even though the pore space may be reduced.[15]

The H_2 adsorption isotherms of MC-BIF-2H, MC-BIF-3H, and MC-BIF-5H at 77 K and 1 atm give an uptake of 9.9, 28.2 and 3.7 cm^3g^{-1}, respectively. Likely due to the small pore aperture in these MC-BIFs, the H_2 adsorption/desorption isotherms of these samples are distinctly hysteretic. Although these compounds showed CO_2 and H_2 adsorption, no significant N_2 adsorption was observed, which is likely due to the limitation of the aperture size.

In summary, we have created a new family of porous materials (MC-BIFs) by integrating metal carboxylates and boron imidazolates. The rich synthetic and structural chemistry of the MC-BIF system has been demonstrated through both hydro- or solvothermal synthesis with different metal ions (Zn^{2+} or Cd^{2+}) and different carboxylates (bdc and btc), in conjunction with $[B(im)_4]^-$ complexes and “free” imidazolate ligand. The dimensionality of M/carboxylate and M/$[B(im)_4]$ substructures can also be tuned to create new framework materials with tunable gas sorption properties. Among these new materials, the hydrothermally synthesized MC-BIF-2H exhibits a very high volumetric CO_2 storage capacity at 81L/L, comparable to 83L/L previously reported for a highly porous ZIF-69.

Supplementary Material

Refer to Web version on PubMed Central for supplementary material.

Acknowledgments

We thank the support of this work by NSF (X. B. DMR-0846958), DOE (P. F. DE-SC0002235), and NIH-RISE (R. N. GM071638). X. B is a Henry Dreyfus Teacher Scholar.

References

1. Long, J.; Yaghi, OM., editors. Chem Soc Rev. Vol. 38. 2009. Topical issue on metal-organic frameworks; p. 1213-1504.
2. Férey G. Chem, Soc, Rev. 2008; 37:191. [PubMed: 18197340]
3. a) Chui SSY, Lo SMF, Charmant JPH, Orpen AG, Williams LD. Science. 1999; 283:1148. [PubMed: 10024237] b Li H, Eddaoudi M, O'Keeffe M, Yaghi OM. Nature. 1999; 402:276.c) Férey G, Mellot-Draznieks C, Serre C, Millange F, Dutour J, Surblé S, Margiolaki I. Science. 2005; 309:2040. [PubMed: 16179475] d) Yang S, Lin X, Blake AJ, Walker G, Hubberstey P, Champness NR, Schröder M. Nat Chem. 2009; 1:487. [PubMed: 21378916] e) Zhao X, Xiao B, Fletcher AJ, Thomas KM, Bradshaw D, Rosseinsky MJ. Science. 2004; 306:1012. [PubMed: 15486255]
4. a) Xiao B, Byrne PJ, Wheatley PS, Wragg DS, Zhao X, Fletcher AJ, Thomas KM, Peters L, Evans JSO, Warren JE, Zhou W, Morris RE. Nature Chem. 2009; 1:289. [PubMed: 21495253] b) Ma L, Jin A, Xie Z, Lin W. Angew Chem. 2009; 121:10089.Angew Chem Int Ed. 2009; 48:9905.c) Koh K, Wong-Foy AG, Matzger AJ. J Am Chem Soc. 2009; 131:4184. [PubMed: 19267435] d) Tsuruoka T, Furukawa S, Takashima Y, Yoshida K, Isoda S, Kitagawa S. Angew Chem. 2009; 121:4833.Angew Chem Int Ed. 2009; 48:4739.
5. a) Chen B, Wang L, Xiao Y, Fronczek FR, Xue M, Cui Y, Qian G. Angew Chem. 2009; 121:508.Angew Chem Int Ed. 2009; 48:500.b) Zhao D, Yuan D, Sun D, Zhou HC. J Am Chem Soc. 2009; 131:9186. [PubMed: 19530682] d) Zhang J, Wojtas L, Larsen RW, Eddaoudi M, Zaworotko MJ. J Am Chem Soc. 2009; 131:17040. [PubMed: 19891485] c) Park HJ, Suh MP. Chem Commun. 2010; 46:610.
6. a) Demessence A, D'Alessandro DM, Foo ML, Long JR. J Am Chem Soc. 2009; 131:8784. [PubMed: 19505094] b) Sumida K, Hill MR, Horike S, Dailly A, Long JR. J Am Chem Soc. 2009; 131:15120. [PubMed: 19799422] c) Zhang YB, Zhang WX, Feng FY, Zhang JP, Chen XM. Angew Chem. 2009; 121:5391.Angew Chem Int Ed. 2009; 48:5287.d) Sonnauer A, Hoffmann F, Fröba M, Kienle L, Duppel V, Thommes M, Serre C, Férey G, Stock N. Angew Chem. 2009; 121:3768.Angew Chem Int Ed. 2009; 48:3791.e) Ahnfeldt T, Guillou N, Gunzelmann D, Margiolaki I, Loiseau T, Férey G, Senker J, Stock N. Angew Chem. 2009; 121:5265.Angew Chem Int Ed. 2009; 48:5163.f) Mulfort KL, Farha OK, Malliakas CD, Kanatzidis MG, Hupp JT. Chem Eur J. 2010; 16:276.
7. a) Alkordi MH, Brant JA, Wojtas L, Kravtsov VC, Cairns AJ, Eddaoud M. J Am Chem Soc. 2009; 131:17753. [PubMed: 19921841] b); c) Li K, Olson DH, Seidel J, Emge TJ, Gong H, Zeng H, Li J. J Am Chem Soc. 2009; 131:10368. [PubMed: 19722614] d) Wu HB, Wang QM. Angew Chem. 2009; 121:7479.Angew Chem Int Ed. 2009; 48:7343.e) Qiu Y, Deng H, Mou J, Yang S, Zeller M, Batten SR, Wue H, Lie J. Chem Commun. 2009:5415.f) An J, Geib SJ, Rosi NL. J Am Chem Soc. 2010; 132:38. [PubMed: 20000664] g) Tian YQ, Yao SY, Gu D, Cui KH, Guo DW, Zhang G, Chen ZX, Zhao DY. Chem Eur J. 2010; 16:1137.
8. a) Lu Z, Knobler CB, Furukawa H, Wang B, Liu G, Yaghi OM. J Am Chem Soc. 2009; 131:12532. [PubMed: 19689142] b) Phan A, Doonan CJ, Uriberomo FJ, Knobler CB, O'Keefee M, Yaghi OM. Acc Chem Res. 2010; 10:58. [PubMed: 19877580]
9. a) Zhang J, Wu T, Zhou C, Chen S, Feng P, Bu X. Angew Chem. 2009; 121:2580.Angew Chem Int Ed. 2009; 48:2542.b) Wu T, Zhang J, Zhou C, Wang L, Bu X, Feng P. J Am Chem Soc. 2009; 131:6111. [PubMed: 19366266]
10. Chen S, Zhang J, Wu T, Feng P, Bu X. Dalton Trans. 2010; 39:697. [PubMed: 20066209]
11. Huang SH, Lin CH, Wu WC, Wang SL. Angew Chem. 2009; 121:6240.Angew Chem Int Ed. 2009; 48:6124.
12. Spek, AL. Platon. Utrecht University; The Netherlands: 2003.
13. Banerjee R, Phan A, Wang B, Knobler C, Furukawa H, O'Keeffe M, Yaghi OM. Science. 2008; 319:939. [PubMed: 18276887]
14. a) Dincă M, Long JR. Angew Chem. 2008; 120:6870.Angew Chem, Int Ed. 2008; 47:6766.b) Wu H, Zhou W, Yildirim T. J Am Chem Soc. 2009; 131:4995. [PubMed: 19275154]
15. a) Ma L, Lin W. Angew Chem. 2009; 121:3691.Angew Chem Int Ed. 2009; 48:3637.b) Chen S, Zhang J, Wu T, Feng P, Bu X. J Am Chem Soc. 2009; 131:16027. [PubMed: 19842698]

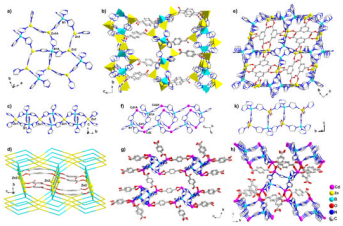

Figure 1.

(a) and (b) View of 2D B/im/Zn layer and 3D structure of MC-BIF-1S, respectively. ZnN_3O tetrahedron: yellow; BN_4 tetrahedron: blue. (c) and (d) View of 1D B/im/Zn chain and 3D structure of MC-BIF-2H, respectively. All 2-connected im ligands were simplified as lines. (e) View of 3D structure of MC-BIF-3H. (f) and (g) View of 1D B/im/Cd tube and 3D structure of MC-BIF-4S, respectively. The neutral Him and p-murea are omitted for clarity. (h) View of 3D structure of MC-BIF-5. (k) 1D double-chain structure in MC-BIF-6S.

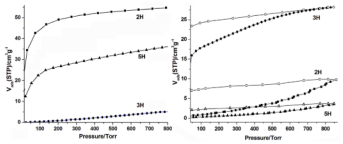

Figure 2.

(a) CO_2 adsorption isotherms of MC-BIF-2H (■), MC-BIF-3H (●) and MC-BIF-5H (▲). (b) H_2, adsorption (■●▲) and desorption (□○△) isotherms of MC-BIF-2H, MC-BIF-3H, and MC-BIF-5H.

Table 1

A Summary of Crystal Data and Refinement Results.[a]

Compound	Formula	Sp. Gr.	*a* (A)	b (A)	c (A)	α (°)	β (°)	γ (°)	*R*(F)
MC-BIF-1S	$[Zn_2(im)(bdc)][B(im)_4]\cdot$p-murea	$P4_32_12$	13.0584(18)	13.0584(18)	53.7310(11)	90	90	90	8.00%
MC-BIF-2H	$[Zn_3(bdc)_2(H_2O)][B(im)_4]_2\cdot 2H_2O$	*C2/c*	13.1669(14)	21.2270(2)	18.2540(2)	90	106.787(7)	90	5.17%
MC-BIF-3H	$[Zn_2(btc)][B(im)_4]\cdot 3H_2O$	$P2_1/c$	11.8587(15)	13.7752(16)	16.7460(2)	90	96.469(7)	90	5.42%
MC-BIF-4S	$[Cd(Him)(p\text{-murea})][Cd(bdc)_{1.5}]$- $[B(im)_4]\cdot$p-murea	*P-1*	9.3195(2)	14.2603(2)	18.4982(4)	105.307(1)	99.077(1)	95.406(1)	3.67%
MC-BIF-5H	$[Cd_2(bdc)(Hbdc)][B(im)_4]\cdot 0.5H_2O$	$P2_1/c$	8.8738(5)	18.3991(9)	20.1384(10)	90	98.843(1)	90	3.22%
MC-BIF-6S	$[Zn(OAC)][B(im)_4]$	Pnma	13.5313(7)	9.9802(5)	12.7491(7)	90	90	90	4.15%

[a] im = imidazolate; bdc = 1,4-benzenedicarboxylate; btc = 1,3,5-benzenetricarboxylate; p-murea = 1,3-dimethyl-propyleneurea; OAC = CH_3COO^-